Pergamon

Journal of Structural Geology, Vol. 17, No. 12, pp. 1771 to 1784, 1995

0191-8141/95 $9.50+0.00

0191-8141(95)00069-0

The limitations of three-dimensional kinematic vorticity analysis

BASIL TIKOFF

Department of Geology and Geophysics, University of Minnesota, Minneapolis, MN 55455, U.S.A.

and

HAAKON FOSSEN

Statoil, GF/PETEK-GEO, N-5020 Bergen, Norway

(*Received* 16 *February* 1994; *accepted in revised form* 15 *June* 1995)

Abstract—The kinematic vorticity number (W_k) can be calculated for three-dimensional as well as two-dimensional geologic deformations. For steady-state deformations, W_k can be correlated to and analyzed in terms of finite strains. The analysis shows that assumptions commonly made for two-dimensional deformations are not applicable to three-dimensional deformations. A single W_k describes an infinite number of three-dimensional deformations. Further, even knowledge of flow apophyses orientation, instantaneous stretching axes orientation, and/or W_k are not sufficient to describe deformation. Three-dimensional deformations also require knowledge of the deformation 'type' or boundary conditions of deformation (e.g. transpression). Hence, in addition to being difficult to estimate, the value of knowing W_k for three-dimensional deformations is greatly reduced compared with plane strain. The most useful methods of determining W_k from naturally deformed rocks are presented.

INTRODUCTION

The kinematic vorticity number (W_k) was first introduced into the geological literature by McKenzie (1979) and Means *et al.* (1980). W_k has its origin in fluid dynamics (Truesdell 1953) and records the amount of rotation relative to the amount of stretching, at a point in space and in an instant in time. Therefore, W_k analyses can distinguish, for example, intermediate cases between pure shear ($W_k = 0$) and simple shear ($W_k = 1$). The application of kinematic vorticity analysis to geologic problems was greatly facilitated by the use of the Mohr circle for strain (Means 1983, De Paor & Means 1984, Passchier 1988a). Using Mohr circle constructions, estimates of W_k from deformed vein sets became possible (Passchier & Urai 1988). Other studies of kinematic vorticity (Vissers 1989, Wallis 1992, Passchier 1990, Simpson & De Paor 1993, Tikoff & Teyssier 1994a) have used increasingly sophisticated methods for determining W_k.

Three-dimensional analyses of both individual shear zones and tectonic settings are becoming more common in the geological literature. Ramberg (1975a,b) and McKenzie (1979) were two early attempts to quantify three-dimensional deformation, although neither specifically includes kinematic vorticity. The three-dimensional kinematic vorticity number can be given in terms of the components of the velocity gradient tensor **L** and, assuming steady-state deformation, the deformation matrix (or position-gradient tensor) **D** (Appendix A), (Tikoff & Fossen 1993). This mathematical framework allows a direct correlation of W_k to the instantaneous stretching axes (ISA), flow apophyses, and finite strain for three-dimensional deformations. Based on this framework, we discuss the use and limitations of the kinematic vorticity number in three dimensions.

Table 1.

Nomenclature

AP_n	Flow apophyses
D	Deformation matrix, position gradient tensor
$\dot{\delta}_i$	Volume change strain rate
Δ	Anisotropic volume change
$\dot{\varepsilon}_i$	Pure shear strain rate
$\dot{\gamma}$	Simple shear strain rate
γ	Shear strain (simple shear component)
Γ	Effective shear strain
ISA	Instantaneous stretching (strain) axis(es)
II	Invariant second moment of the stretching tensor
k_n	Stretches along coordinate axes
λ_n	Quadratic principal stretches of the finite strain ellipsoid, eigenvalues of the matrix $\mathbf{DD}^{\mathrm{T}}$
$\mathbf{DD}^T$	Finger tensor, for calculating finite strain
L	Velocity gradient tensor
$\dot{\mathbf{S}}$	Stretching tensor
$\dot{s}_1, \dot{s}_2, \dot{s}_3$	Principal stretching (strain) rates, eigenvalues of matrix $\dot{\mathbf{S}}$; magnitudes of ISA
θ	Angle between the long axis of instantaneous strain (ISA) and the x-coordinate axis
θ'	Angle between the long axis of the finite strain ellipse and the x-coordinate axis
v	Velocity vector
W	Vorticity tensor
w	Vorticity vector
w	Magnitude of the vorticity vector
ω	Local angular velocity vector
ω	Magnitude of angular velocity vector
W_k	Kinematic vorticity number, general vorticity
W_{k_e}	Kinematic vorticity number, external vorticity
W_{k_i}	Kinematic vorticity number, internal vorticity
z	Vertical coordinate axis

KINEMATIC VORTICITY NUMBER (W_k)

Origin and definition

The kinematic vorticity number (Truesdell 1953) is defined in a fluid that flows with a velocity **v** which varies in space. The *vorticity* is the vector defined as $\mathbf{w} = 2\omega$ (angular velocity vector) = curl **v**. Thus, the vorticity vector **w** is parallel to the angular velocity vector ω and has twice its magnitude. The angular velocity ω may be interpreted as: (1) the average rotation of all lines in the plane perpendicular to **v**; (2) the rate of rotation of a set of material lines that are parallel to the instantaneous stretching axes (ISA) with respect to the ISA; (3) the average rate of rotation of any two perpendicular material lines in the plane perpendicular to **v**; or (4) the rate of rotation of a rigid spherical inclusion in a ductile matrix (strictly true only for a particle with no slip along its boundaries and infinitely high viscosity contrast) (Means *et al.* 1980, Ghosh 1987).

The vorticity indicates both the direction and rate of rotation of the fluid at a point. To understand what vorticity physically represents, one can imagine a spherical element of the fluid that suddenly freezes while the surrounding fluid disappears (Kreyszig 1972, p. 621). What would remain is a small sphere of (frozen) fluid which rotates with an angular velocity ω at that point in space (Fig. 1). The vorticity vector would be the axis about which the fluid sphere is revolving most rapidly, and its magnitude (or length) indicates the rate of rotation at that point.

In search for a dimensionless measure of the non-coaxiality of deformation, Truesdell (1953) pointed out that it must be a ratio between the 'rotation' and the 'pure deformation' (or change of shape) involved. The latter is conveniently described by the principal stretching rates $\dot{s}_1$, $\dot{s}_2$ and $\dot{s}_3$ which are the eigenvalues of the stretching tensor $\dot{\mathbf{S}}$ (Appendix A). Therefore, the kinematic vorticity number W_k was defined as

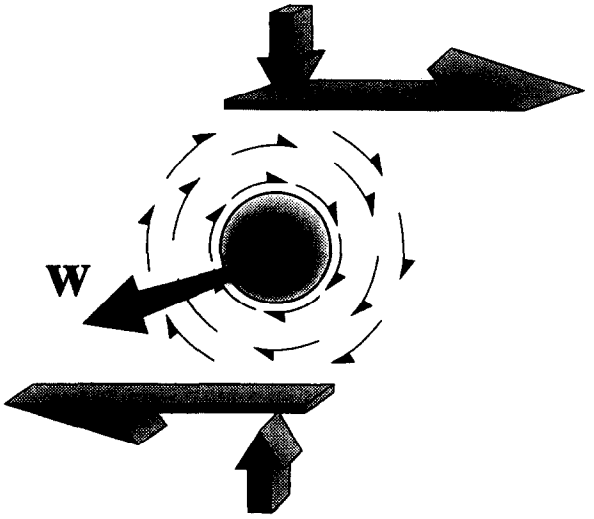

Fig. 1. Illustration of the vorticity vector (**w**) and its relation to a rotating rigid sphere with no slip along its boundaries in a deforming rock.

$$W_k = \frac{w}{\sqrt{2(\dot{s}_1^2 + \dot{s}_2^2 + \dot{s}_3^2)}} = \frac{2\omega}{\sqrt{2(\dot{s}_1^2 + \dot{s}_2^2 + \dot{s}_3^2)}}. \quad (1)$$

For irrotational deformations, such as pure shear, the numerator in equation (1) goes to zero and $W_k = 0$. For a rigid rotation with no stretching, the denominator in equation (1) goes to zero and the deformation is characterized by $W_k = \infty$. $W_k > 1$ correlates to pulsating deformation histories (Ramberg 1975a), while simple shearing deformations are described by $W_k = 1$. Notice that W_k does not record rate of rotation, but rather 'quality' of rotation (Ghosh 1987). W_k describes, instantaneously, how fast the stretching of the ISA occurs with respect to overall rotation, with respect to an external reference frame.

Conventions for W_k *analyses*

Any velocity field can be decomposed into three components: (1) rate of translation; (2) rate of stretching; and (3) rate of rotation (Truesdell 1953, Lister & Williams 1983). We will assume that translation can be treated separately and will not address this aspect of deformation. Generally, the rotation component defines the vorticity and the stretching component defines the instantaneous stretching (or strain) axes. However, we can further partition the vorticity into (1) shear-induced or internal vorticity (W_{k_i}), which is caused by a non-coaxial component of deformation; and (2) spin or external vorticity (W_{k_e}), which results in rotation of the instantaneous strain (or stretching) axes through an external reference frame (Means *et al.* 1980). Kinematic vorticity thus incorporates both the internal and the external spin of the system (Lister & Williams 1983):

$$W_k = f(W_{k_i}, W_{k_e}, \text{rigid body rotation}). \quad (2)$$

Consequently, W_k is a Lagrangian concept. That is, to truly quantify the type of deformation, one must choose an external reference frame and quantify deformation in this context. In contrast, most field geology is, by necessity, Eulerian. Commonly used vorticity criteria, such as porphyroblast or crystallographic fabric studies (see below), only record internal vorticity (W_{k_i}). With these criteria, we may be able to determine the amount of internal stretching vs rotation at a single outcrop, but we are unlikely to be able to determine the amount of larger-scale external spin. Hence, as we try to relate vorticity to rocks, we will concentrate on the internal vorticity W_{k_i}. Upper triangular velocity-gradient and position-gradient tensors, such as presented in this paper, inherently contain only shear-induced or internal vorticity, and are therefore used in the following discussion of three-dimensional strain.

Throughout this analyses, we have chosen to use the flow apophyses parallel to the x-axis as our reference frame, following Weijermars (1991) and Simpson & De Paor (1993). In order to apply this reference frame to a field study, one must assume that the x-axis parallels the shear zone boundary. However, if this assumption holds, one can easily model non-steady-state defor-

mations, using the same reference plane, since the x-parallel flow apophysis remains fixed. Further, the flow apophyses have some physical meaning for finite, as well as instantaneous, strain. Generally, the long axis of the finite strain ellipsoid rotates into parallelism with one of the flow apophyses, a situation which is easy to visualize for plane strain deformations.

Notice that other reference frames are also possible. Passchier (1988b) chooses to define his coordinate system with respect to the ISA, because the ISA remain perpendicular and fixed in space throughout a steady-state deformation. However, since the orientation of the ISA and flow apophyses are fixed with respect to each other, either choice is acceptable.

DEFORMATION THEORY

For any deformation, the kinematics are defined instantaneously by the velocity field given by the velocity gradient tensor **L** (Means 1990). The most general three-dimensional velocity field is given by

$$\mathbf{L} = \begin{pmatrix} \dot{\varepsilon}_x & \dot{\gamma}_{xy} & \dot{\gamma}_{xz} \\ \dot{\gamma}_{yx} & \dot{\varepsilon}_y & \dot{\gamma}_{yz} \\ \dot{\gamma}_{zx} & \dot{\gamma}_{zy} & \dot{\varepsilon}_z \end{pmatrix}. \tag{3}$$

Equation (3) includes internal vorticity, external vorticity, and rigid body rotation. The corresponding kinematic vorticity number can thus be written as (Appendix A):

$$W_k = \frac{\sqrt{(\dot{\gamma}_{zy} - \dot{\gamma}_{yz})^2 + (\dot{\gamma}_{xz} - \dot{\gamma}_{zx})^2 + (\dot{\gamma}_{yx} - \dot{\gamma}_{xy})^2}}{\sqrt{2(\dot{\varepsilon}_x^2 + \dot{\varepsilon}_y^2 + \dot{\varepsilon}_z^2) + [(\dot{\gamma}_{xy} + \dot{\gamma}_{yx})^2 + (\dot{\gamma}_{xz} + \dot{\gamma}_{zx})^2 + (\dot{\gamma}_{yz} + \dot{\gamma}_{zy})^2]}}. \tag{4}$$

While this may be useful in certain applications, such as computational modeling, geologists rarely have the ability to evaluate external vorticity and rigid body rotation. Therefore, we would like to have a relation that expresses only internal vorticity.

A general, non-spinning, three-dimensional deformation that combines a general coaxial deformation, with or without volume loss, and any of the three orthogonal simple shears whose movement is parallel to a coordinate axis (see Tikoff & Fossen 1993), a velocity gradient tensor is given by

$$\mathbf{L} = \begin{pmatrix} \dot{\varepsilon}_x & \dot{\gamma}_{xy} & \dot{\gamma}_{xz} \\ 0 & \dot{\varepsilon}_y & \dot{\gamma}_{yz} \\ 0 & 0 & \dot{\varepsilon}_z \end{pmatrix}, \tag{5}$$

where $\dot{\varepsilon}_i$ are the pure shear strain rates and $\dot{\gamma}_i$ are the simple shear strain rates. Anisotropic volume loss can be incorporated into the above tensor by substituting into the pure shear strain rates (Sanderson 1976, Fossen & Tikoff 1993). Upper triangular matrices do not contain an external spin component and record only internal vorticity.

The deformation matrix **D** that corresponds to the velocity gradient tensor **L** given in equation (5) can be expressed as equation (6) (Tikoff & Fossen 1993) and the related internal kinematic vorticity number is

$$W_{k_i} = \frac{\sqrt{(\dot{\gamma}_{yz})^2 + (\dot{\gamma}_{xz})^2 + (\dot{\gamma}_{xy})^2}}{\sqrt{2(\dot{\varepsilon}_z^2 + \dot{\varepsilon}_y^2 + \dot{\varepsilon}_z^2) + (\dot{\gamma}_{xy})^2 + (\dot{\gamma}_{xz})^2 + (\dot{\gamma}_{yz})^2}}. \tag{7}$$

Merle (1986) showed that steady-state deformations could be put into time-independent solutions. Using the relations

$$\dot{\gamma}_{xz} = \gamma_{xz}/t, \quad \dot{\gamma}_{yz} = \gamma_{yz}/t, \quad \dot{\gamma}_{xy} = \gamma_{xy}/t,$$

and

$$\exp(\dot{\varepsilon}_x t) = k_x, \quad \exp(\dot{\varepsilon}_y t) = k_y, \quad \exp(\dot{\varepsilon}_z t) = k_z,$$

and for unit time:

$$\begin{aligned} \dot{\varepsilon}_x &= \ln k_x, \quad \dot{\varepsilon}_y = \ln k_y, \quad \dot{\varepsilon}_z = \ln k_z, \\ \dot{\gamma}_{xz} &= \gamma_{xz}, \quad \dot{\gamma}_{yz} = \gamma_{yz}, \quad \dot{\gamma}_{xy} = \gamma_{xy}, \end{aligned} \tag{8}$$

we can write a time-independent solution of the deformation tensor

$$\mathbf{D} = \begin{bmatrix} k_x & \Gamma_{xy} & \Gamma_{xz} \\ 0 & k_y & \Gamma_{yz} \\ 0 & 0 & k_z \end{bmatrix}, \tag{9a}$$

where

$$\Gamma_{xy} = \frac{\gamma_{xy}(k_x - k_y)}{\ln(k_x/k_y)}, \tag{9b}$$

$$\Gamma_{xz} = \frac{\gamma_{xz}(k_x - k_z)}{\ln(k_x/k_z)} + \frac{\gamma_{xy}\gamma_{yz}(k_x - k_y)}{\ln(k_x/k_y)\ln(k_y/k_z)} + \frac{\gamma_{xy}\gamma_{yz}(k_z - k_x)}{\ln(k_x/k_z)\ln(k_y/k_z)}, \tag{9c}$$

$$\Gamma_{yz} = \frac{\gamma_{yz}(k_y - k_z)}{\ln(k_y/k_z)} \tag{9d}$$

(Tikoff & Fossen 1993); k_x, k_y and k_z represent the finite stretches along the x-, y- and z-coordinate axes (includes volume change if $k_x k_y k_z \neq 1$), and the off-diagonal terms (Γ) represent elements of shear deformation. If we consider a left-handed coordinate system, Γ_{xy} reflects a wrench in the x-direction, and Γ_{xz} and Γ_{yz} correspond to thrusts in the x- and y-directions, respectively. The eigenvalues and eigenvectors of the matrix $\mathbf{DD}^T$ give the

$$\mathbf{D} = \begin{bmatrix} \exp(\dot{\varepsilon}_x t) & \dfrac{\dot{\gamma}_{xy}\{\exp(\dot{\varepsilon}_x t) - \exp(\dot{\varepsilon}_y t)\}}{(\dot{\varepsilon}_x - \dot{\varepsilon}_y)} & \dfrac{\dot{\gamma}_{yz}\dot{\gamma}_{xy}\{\exp(\dot{\varepsilon}_x t) - \exp(\dot{\varepsilon}_y t)\}}{(\dot{\varepsilon}_x - \dot{\varepsilon}_y)(\dot{\varepsilon}_y - \dot{\varepsilon}_z)} + \dfrac{\dot{\gamma}_{yz}\dot{\gamma}_{xy}\{\exp(\dot{\varepsilon}_z t) - \exp(\dot{\varepsilon}_x t)\}}{(\dot{\varepsilon}_y - \dot{\varepsilon}_z)(\dot{\varepsilon}_x - \dot{\varepsilon}_z)} + \dfrac{\dot{\gamma}_{xz}\{\exp(\dot{\varepsilon}_x t) - \exp(\dot{\varepsilon}_z t)\}}{(\dot{\varepsilon}_x - \dot{\varepsilon}_z)} \\ 0 & \exp(\dot{\varepsilon}_y t) & \dfrac{\dot{\gamma}_{yz}\{\exp(\dot{\varepsilon}_y t) - \exp(\dot{\varepsilon}_z)\}}{(\dot{\varepsilon}_y - \dot{\varepsilon}_z)} \\ 0 & 0 & \exp(\dot{\varepsilon}_z t) \end{bmatrix} \tag{6}$$

magnitude and orientation of the finite strain ellipsoid (e.g. Flinn 1979).

If we assume a steady-state deformation, we can use the same relations [equation (9)] for three-dimensional kinematic vorticity to finite strain. Under these special conditions, W_{ki} remains constant during deformation. Therefore, W_{ki}—by definition an instantaneous quantity [equation (1)]—can be expressed in terms of finite strain values:

$$W_{k_i} = \frac{\sqrt{(\gamma_{yz})^2 + (\gamma_{xz})^2 + (\gamma_{xy})^2}}{\sqrt{2[\ln(k_1)^2 + \ln(k_2)^2 + \ln(k_3)^2] + (\gamma_{xy})^2 + (\gamma_{xz})^2 + (\gamma_{yz})^2}}. \quad (10)$$

Similarly, one can express **L** [equation (5)], the orientation of the flow apophyses and the orientation of the ISA in time-independent terms.

Most geological applications have used two-dimensional W_k estimates (e.g. Means *et al.* 1980, Bobyarchick 1986, Passchier 1990, Weijermars 1991). The above analysis is simply an extension of these earlier analyses into three dimensions. Robin & Cruden (1994) use a 'sectional' W_k value, which calculates W_k in a (two-dimensional) section for a three-dimensional deformation. For the special case of plane strain, the internal kinematic vorticity number can be expressed as

$$W_{k_i} = \cos[\arctan(\ln(k_x/k_y)/\gamma)] \quad (11)$$

and the acute angle α between the two flow apophyses as

$$\alpha = \arctan[\ln(k_x/k_y)/\gamma] \quad (12)$$

(Tikoff & Fossen 1993), where

$$W_{k_i} = \cos\alpha \quad (13)$$

Bobyarchick (1986). The simple relationship between flow apophyses and ISA for plane strain is given by

$$\alpha = 90 - 2\theta \quad (14a)$$

and

$$\alpha' = 2\theta \quad (14b)$$

(Weijermars 1991) where α' is the angle between the oblique flow apophyses and the y-axis. The relationships between α, α', θ and W_{k_i} are shown graphically in Fig. 2.

These relationships are more complex for three-dimensional deformations, as no simple relationship exists between W_{k_i} and α, α' and θ. Hence, the relation between W_{k_i} and the ISA given by

$$W_{k_i} = \cos(90 - 2\theta) \quad (15)$$

(Bobyarchick 1986) only holds for plane strain deformations.

THREE-DIMENSIONAL W_k ANALYSIS

An intuitive understanding of three-dimensional vorticity is not straightforward. The extension of kinematic vorticity from two dimensions to three dimensions is easy to visualize for cases where one of the three ISA is non-rotating. In this case, the vorticity vector becomes parallel to the non-rotating ISA. In the general case, the interpretation of the vorticity vector becomes more abstract, but the vorticity vector (**w**) is always perpendicular to the plane containing the maximum rotation. For general three-dimensional strain, **w** will not have any predetermined orientation with respect to the ISA, unlike simple shear where **w** is parallel to the shear zone and perpendicular to the shear direction.

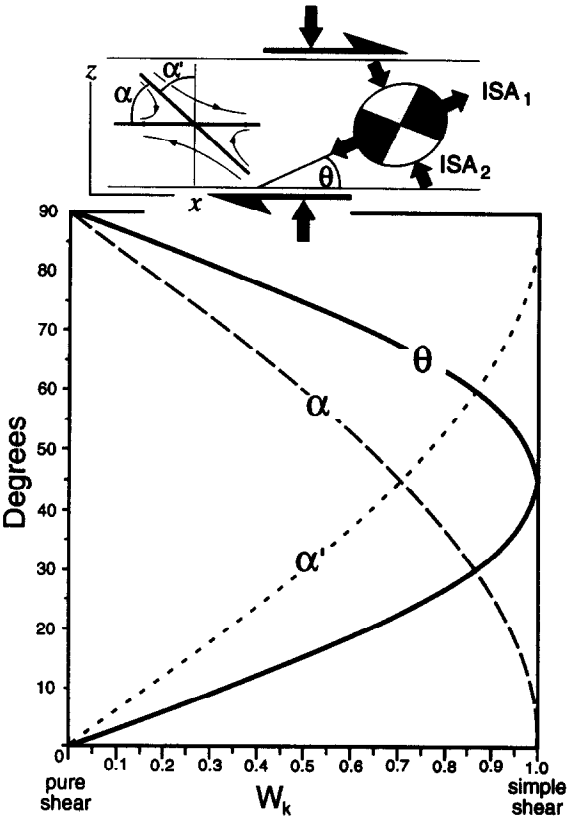

Fig. 2. The relationship of W_{k_i} with the acute angle (α) between the flow apophyses, angle between the oblique flow apophysis and the normal to the deformation zone (α') and with the orientation of the ISA (instantaneous stretching axes); θ defines the angle between the extensional ISA and the boundaries of the deformation zone.

Unlike plane strain deformation (Fig. 2), the orientation for flow apophyses and/or the ISA does not define a unique kinematic vorticity for three-dimensional deformation. In other words, there is no relationship between the orientation of the flow apophyses and W_{k_i}. Figure 3 shows three separate deformations: (a) plane strain deformation; (b) flattening and a simple shear; and (c) transpression. These fundamentally different deformations can all lead to identical orientations of the flow apophyses and ISA, but with different W_{k_i} values. Further, the three aforementioned cases are all 'end-members' of deformational histories and an infinite number of 'intermediate' deformations will cause the same orientation of flow apophyses and ISA.

These results highlight a serious problem with W_k analyses: a given W_{k_i} represents an infinite number of deformations. Therefore W_{k_i}, by itself, is not sufficient for describing particle movement or flow during deformation. In two-dimensional, plane strain deformation, the same kinematic vorticity number could refer to

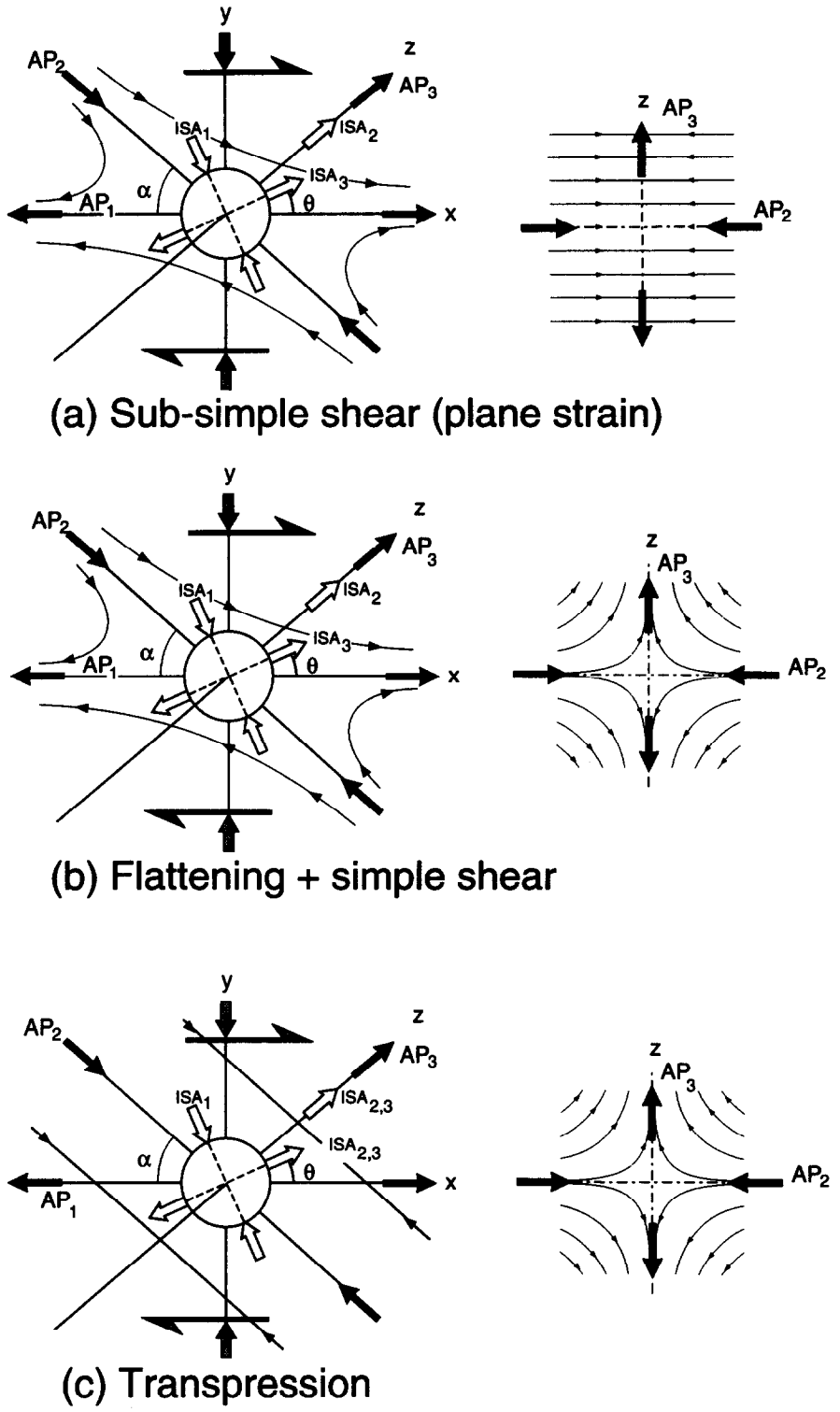

Fig. 3. Orientations of flow apophyses (black arrows), ISA (white arrows) and flow lines (light lines) for three three-dimensional deformations. The right diagrams depicts flow in AP_2–AP_3 plane. Each case corresponds to a different W_k value.

either a pure shear shortening or extension along the x-direction (e.g. Weijermars 1991, Simpson & De Paor 1993). This problem is exacerbated in three dimensions, where even with a known, single simple shear direction, a given W_{k_i} could indicate a constrictional, flattening, transpression, plane strain, or an infinite variety of intermediate types of deformation. Therefore, a single, three-dimensional W_{k_i} describes an infinite number of deformations and can not uniquely define a deformation.

Another problem that is specific to three-dimensional W_k analysis regards its relation to other instantaneous strain quantities. For plane-strain deformations, the orientation of the flow apophyses or ISA uniquely defines W_{k_i}. This is not true for three-dimensional deformation. Here, the orientation of the flow apophyses

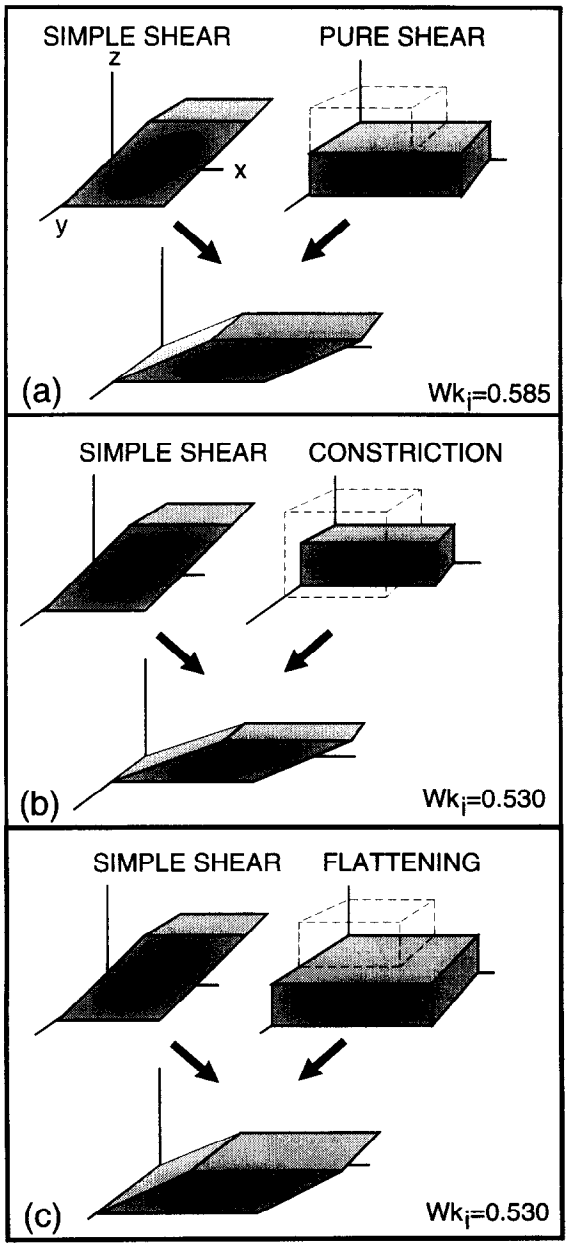

Fig. 4. (a) Plane strain; (b) constriction with simple shear; and (c) flattening with simple shear deformations that result in an identical finite strain ellipse in the x–z plane; W_{k_i} is lower for the flattening/constriction cases (b,c) due to the greater non-coaxial component.

and/or ISA cannot, without knowledge of 'type' of deformation (e.g. general flattening combined with shearing; Fig. 4c), be used to calculate W_{k_i}. Notice that the reverse is also true: different 'types' of deformation (such as those in Fig. 3) could have the same W_{k_i}, but each would result in different orientations of the ISA and flow apophyses. To calculate W_{k_i} for three-dimensional deformations, a qualitative description of the type of deformation *and* the orientation of the ISA or flow apophyses (or finite strain for steady-state deformations) are necessary.

If one could determine W_k, the orientation of the ISA (or flow apophyses), *and* the magnitude of the ISA (or flow apophyses), the three-dimensional deformation could be uniquely determined. However, since rates of deformation in geological materials are very difficult to assess, this method is unlikely to be usable by structural geologists.

Consequences of treating three-dimensional deformations in two dimensions

Because vorticity has mostly been treated in two dimensions in the literature, a brief three-dimensional example is given here. Consider the case of a single simple shear acting simultaneously with a three-dimensional coaxial deformation (Figs. 4b & c). In this situation, the kinematic vorticity number, in terms of finite deformation parameters, simplifies to

$$W_{k_i} = \frac{\gamma_{xz}}{\sqrt{2[\ln(k_1)^2 + \ln(k_2)^2 + \ln(k_3)^2] + (\gamma_{xz})^2}}. \quad (16)$$

We would like to know how a three-dimensional component of deformation would modify the results of a two-dimensional approximation of W_{k_i} (Appendix B). For two dimensions, let us consider a pure shear deformation ($k_1 = 2$, $k_2 = 1$ and $k_3 = 0.5$) combined with a simple shear component $\gamma = 1$ (Fig. 4a). Substituting these values into equation (16), we find that this deformation produces a $W_{k_i} = 0.585$. We would then like to know how a third coaxial component of deformation would alter the W_{k_i} value, for a constant magnitude of the finite strain ellipse in the x–z plane. To investigate this effect, we require that the same deformation occurs in the x–z plane—namely, a pure shear component of 4:1 ($k_1/k_3 = 4$) combined with a simple shear component of $\gamma_{xz} = 1$. Since we are assuming no volume loss, $k_1k_2k_3 = 1$; k_1 is horizontal and in the shear direction (x-axis), k_2 is horizontal and perpendicular to the shear direction (y-axis) and k_3 is vertical (z-axis; Fig. 4). The magnitude of k_2 determines whether one gets constrictional (Fig. 4b) or flattening (Fig. 4c) strain.

The calculations are shown in Appendix B. In all three cases, the vorticity vector (**w**) is parallel to the y-axis. For an identical finite strain ellipse in the x–z plane, both constriction and flattening require an identical $W_{k_i} = 0.530$, which is lower than the W_{k_i} of the plane strain example ($W_{k_i} = 0.585$). Since $W_{ki} = 0$ for any three-dimensional, coaxial deformation, a lower kinematic vorticity number means that the coaxial component of deformation is more dominant. The extra coaxial component in the flattening and constrictional deformations counteracts the vorticity (**w**) and should therefore reduce W_{k_i}. A more visual approach is to consider the case of material lines during these deformations. The material lines will rotate less as they become oriented closer to the intermediate flow apophysis or y-axis.

There is a substantial effect of the third dimension on estimates of W_{k_i}. Generally, when making field measurements, plane strain deformation is assumed but not conclusively demonstrated. Any vorticity analysis done in two dimensions will tend to overestimate the actual, three-dimensional, kinematic vorticity number, although the error caused by assuming plane strain in the example above should not be greater than ca. 0.05 (Fig.

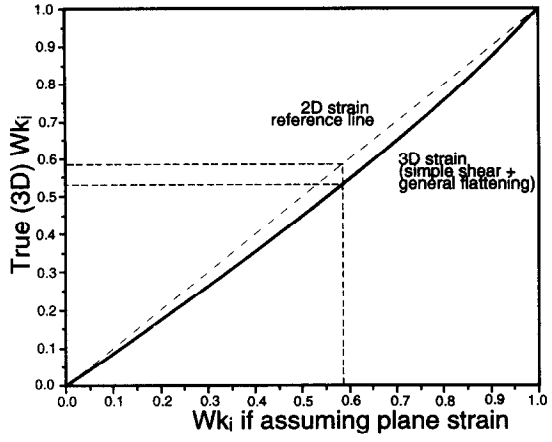

Fig. 5. The difference between the two- and three-dimensional W_{k_i} values for deformations shown in Fig. 4. If plane strain is assumed for a three-dimensional deformation, a W_{k_i} error of 0.05 is possible.

5). Three-dimensional effects should, therefore, be included, if possible, in estimates of W_{k_i}.

The W_{k_i} value of simple shear with flattening and simple shear with constriction are identical, since the kinematic vorticity number simply records, in a non-linear manner, the relative magnitudes of the k and γ values. In order to achieve a 4:1 coaxial strain component in the x–z plane, constrictional or flattening strain must express an equal amount of coaxial deformation in the y-direction (Fig. 4). The only distinction is that the coaxial deformation in the y-direction flows inward in constriction and outward in flattening. The direction of flattening or constriction also does not affect W_{k_i}, analogous to the two-dimensional case. The maximum elongation direction of the coaxial component, in the case of constriction, or maximum shortening direction, in the case of flattening, could be parallel to the x-, y-, or z-axis and would not affect W_{k_i} (although some cases would affect the finite strain in the x–z plane).

Stress and vorticity analysis

Weijermars (1991) suggests that vorticity analysis can indicate the direction of paleostress involved with ductile deformation. Since a vorticity analysis would indicate the orientation of the flow apophyses and instantaneous strain, the stress axes were simply assumed to be parallel to the ISA. While there is nothing incorrect about the analysis, its limitations were not emphasized. In particular, the use of stress introduces several assumptions, the most critical being use of a rheology, in this case a Newtonian viscosity. Very few materials, especially geological materials, act with a linear relationship between stress and strain rate of Newtonian fluids (Kirby & Kronenberg 1987). Further, strain softening or strain hardening, common in natural deformations (White *et al.*, 1980, Neurath & Smith 1982), may change the rheology. Therefore, not only is an assumption of steady-state deformation required, but also one of steady-state rheology. Consider, for example, a ductile shear zone that undergoes strain softening during a simple shear deformation. In this case, the kinematics are still predictable, but the stress-strain rate relationship is not. The use of stress will ultimately limit, rather than expand, vorticity analysis.

Another limitation of Weijermars's stress analysis is that only plane strain deformation is considered. When one considers three-dimensional deformation, or even volume loss combined with pure and simple shearing, the unique relationship between flow apophyses (or ISA) and W_{k_i} does not exist, i.e. the ISA (or stress axes) orientation does not uniquely determine deformation. The only way to quantify three-dimensional deformation is through complete description of the kinematics.

Often, in geological studies, we contend that stresses are the principal cause of the kinematics. However, even with a known (and simple) rheology and homogeneous deformation, this relation is not true. The deformation and vorticity that result from identical orientation of the stress axes are significantly different in each case (e.g. Fig. 3). The tectonic boundary conditions that cause, for example, transpression vs other three-dimensional deformations are potentially as important to the subsequent deformation as the orientation of the ISA (or stress axes). A qualitative description of deformation type—such as three-dimensional flattening strain combined with a simple shear—must accompany calculation of the stress axes (or ISA) orientation or calculation of W_k, if deformation is to be defined. The often overlooked role of boundary conditions plays a significant role in determining kinematics in three-dimensional deformations.

A more philosophical consideration is that stress simply is never recorded in rocks. Any indicator of stress—such as borehole breakout, mineral recrystallization, dike injection, etc.—inherently records a *strain*, albeit a small one in some cases. It is more appropriate to describe these 'stress' features as indicators of either instantaneous strain or small, incremental, finite strain. In even the most straightforward cases, an extra step of interpretation is necessary to calculate stresses from geologic materials. In less straightforward cases, such as stress indicators in anisotropic rock, stress analyses are highly questionable, although deformation analyses (cf. Dennis & Secor 1990) are still applicable and useful.

Pure shear 'bias' of W_{k_i}

Because the three-dimensional deformation tensor [equation (9)] is divided into three pure shear components and three simple shear components, we can investigate the relative roles of these parameters on estimates of W_{k_i}. First, consider a case of plane strain, sub-simple shearing deformation (e.g. Simpson & DePaor 1993). As shown in equation (10), W_{k_i} can be thought of as a non-linear ratio of the pure shear and simple shear components of deformation, assuming a steady-state deformation. It is this non-linearity that

'biases' the W_{ki} value toward the pure shear component in two separate ways.

Since we are interested in the response of material, we can compare the orientation of the ISA for pure shearing ($\theta = 0°$) and simple shearing ($\theta = 45°$). The exactly intermediate case between pure and simple shearing would have a maximum axes of the instantaneous strain oriented at $\theta = 22.5°$. As can be seen, this occurs at $W_{k_i} = 0.75$ (Fig. 2). All $W_{k_i} < 0.75$ are more affected by the pure shear component of deformation. Therefore, a $W_{k_i} = 0.5$ does not imply equal components of pure and simple shearing, but rather that the pure shear component dominates the deformation.

The other way that W_{k_i} is 'biased' toward the pure shear component concerns how strain accumulates during progressive deformation. The pure shear component accumulates efficiently due to its coaxial nature, while simple shear is the least efficient way of accumulating realistic finite strain (Pfiffner & Ramsay 1982). This is shown in Fig. 6, where the pure shear component is shown to grow substantially faster than the simple shear component. Therefore, a deformation with a constant W_{k_i} between 1 and 0.75, although instantaneously more influenced by the simple shear component, will record a strain that increasingly reflects the pure shear component of deformation.

This pure shear 'bias' also applies to three-dimensional deformations. Figure 7(a) shows the orientation of the three principal strain-rates ($\dot{s}_1, \dot{s}_2$ and $\dot{s}_3$) for a transpressional deformation, a combination of vertical stretching compensated by horizontal contraction and an orthogonal simple shear. The pure shear component of deformation extends material in the vertical direction, causing the direction of $\dot{s}_1$ to be vertical. The simple shear component acts orthogonal to the pure shear component, and causes the direction of $\dot{s}_1$ to be horizontal. The switch between the two cases occurs at $W_{k_i} = 0.81$. Therefore, as for the sub-simple shearing case, a $W_{k_i} = 0.5$ implies that the pure shear component dominates the deformation. Additionally, the pure shear component dominates the *finite* deformation, so for transpressional deformations in which $1 > W_{k_i} > 0.81$, the long axis of the finite strain ellipsoid eventually becomes vertical. This effect is discussed in greater detail in Tikoff and Teyssier (1994b) and Fossen *et al.* (1994).

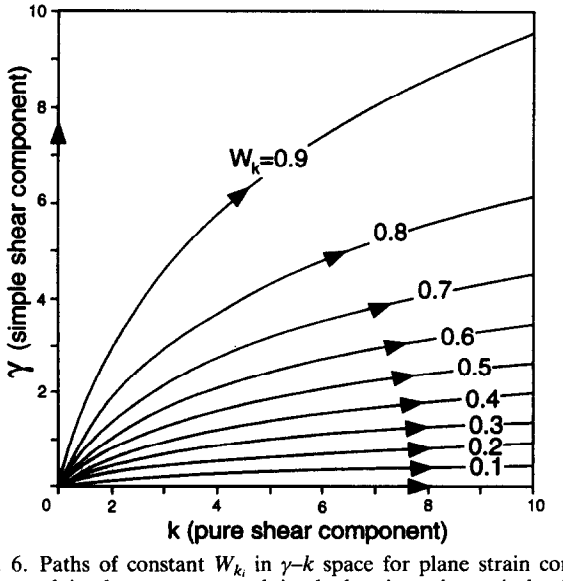

Fig. 6. Paths of constant W_{k_i} in γ–k space for plane strain combinations of simultaneous pure and simple shearing, where γ is the shear strain and k is the pure shear component. Non-linearity of W_{k_i} paths is a result of the finite strain caused by the pure shear component increasing faster than that caused by the simple shear component.

PRACTICAL WAYS OF FINDING W_k IN NATURALLY DEFORMED ROCKS

The above discussion shows that considerable complexities are involved in three-dimensional W_k analyses, and that W_{k_i} alone is not a good measure of three-dimensional deformations. All of the currently used methods of finding W_{k_i} from rocks assume plane strain deformation or very simple three-dimensional deformations. The following sections summarize the most useful methods. Although most of these methods are two-dimensional, they can in principle be modified to cover certain three-dimensional deformations, in which case the methods are restricted to the particular type of deformation in question and cannot be generalized very easily.

In principle, any fabric or structure that reveals some aspect of the deformation history in a rock may be used to extract or approach the average kinematic vorticity in a rock. Elliott (1972, p. 2628) defined three possible measures of non-coaxiality that can be used in structural geology. These are: (1) the orientation and magnitude of the finite and instantaneous strain axes; (2) the orientation and magnitude of two finite strain ellipses that record different amounts of the steady-state deformation; and (3) the rate at which material lines rotate to become parallel to the ISA. It is generally the latter which is considered in mathematical treatments (e.g. Means *et al.* 1980, Lister & Williams 1983).

Simpson & De Paor (1993) define an additional possible reference, namely that of the shear zone boundary (i.e. flow apophyses). That is, assuming that the shear zone boundary parallels one of the flow apophyses, one can use the orientation of the other flow apophyses to define the vorticity [equation (14)]. While this method may be the most applicable to measuring vorticity in the field, it needs rigorous testing before use. It is unclear whether theoretical quantities such as flow apophyses and maximum shear strain rates will necessarily correspond to physical structures such as shear zone boundaries and shear band orientations (Bobyarchick 1986). Heterogeneities within a given rock (e.g. inclusions, stiff layers, pre-existing anisotropy) may be more important in controlling shear band orientation than the flow apophyses or maximum shear strain directions.

Any of the above four measures of non-coaxiality are completely equivalent ways of treating W_{k_i} and the choice should be constrained by the particular setting.

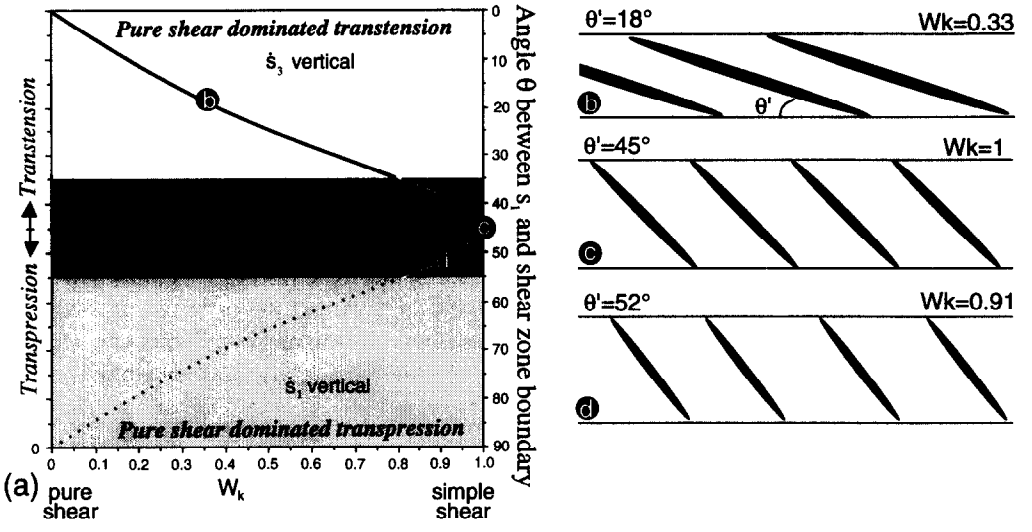

Fig. 7. The W_{k_i} estimates from en échelon tension fracture orientation in transtensional/transpressional setting (based loosely on Jackson & Sanderson 1991). (a) Graph relating ISA orientation to W_{k_i} (Fossen & Tikoff 1993); (b)–(d) en échelon tension fracture arrays, whose extent defines orientation of shear zone. En échelon tension fracture arrays should not form above 55° for transtension/transpression.

Deformed markers in shear zones

In some shear zones, the finite strain ellipsoid can be calculated from deformed markers in sections perpendicular to the shear zone and parallel to the shear direction (lineation). Combined with the angle between the long axis of the finite strain ellipsoid and the shear direction, W_{k_i} can be found. Using an example of sub-simple shearing (Fig. 8a), a finite strain ellipse oriented at 23° to the shear zone boundary with an aspect ratio of 2.0 implies a steady state deformation of $W_{k_i} = 0.9$ (Fig. 9). The critical assumption is that of steady-state flow and the type of deformation. If the shear zone has a 'perfect' geometry, i.e. parallel boundaries and undeformed walls, simultaneous simple shear and volume change may be assumed, and Fig. 8(b) is appropriate. If pure shear, simple shear and volume change were all active, then the volume change must be calculated independently, e.g. from chemical analyses, and equation (11) should be applied.

Figure 8 can also be used for solving the case of two finite strain ellipses with different orientations and magnitudes. Using any two finite strain ellipse magnitudes and the angular relation between them, a unique W_{k_i} value could be defined. This type of example does not require knowledge of, but would indicate, the orientation of the shear zone boundary. For example, the $R = 1$ intercept of the $W_{k_i} = 0.9$ line would indicate the orientation of the ISA and, consequently, the flow apophyses (shear zone boundary) (Fig. 8a). Similarly, one can use Fig. 8 if the orientation of ISA (32° in this case; Fig. 9) or flow apophyses (Fig. 2), relative to the shear zone boundary, is available. Alternatively, one could also use the orientation of the ISA and any finite strain ellipse, using Fig. 8, if the shear zone boundary was unknown.

If several measurements of finite strain can be obtained, the steady-state condition can be tested. If a shear zone responded to steady-state deformation, the

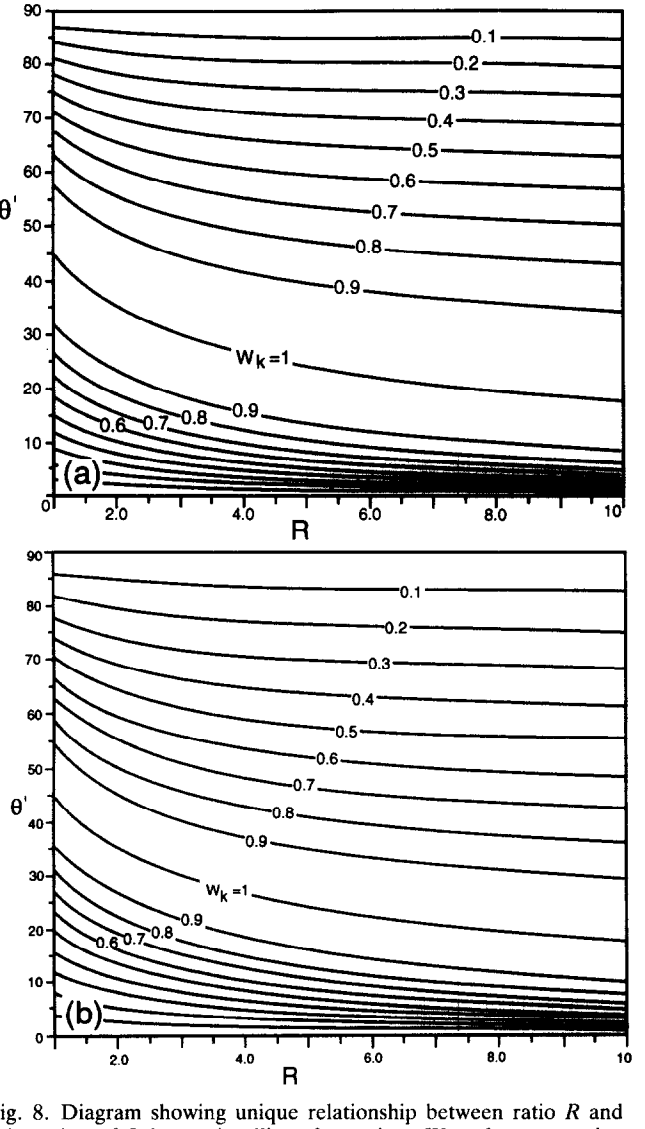

Fig. 8. Diagram showing unique relationship between ratio R and orientation of finite strain ellipse for various W_{k_i} values, assuming steady-state (a) sub-simple shearing; and (b) anisotropic volume loss in y-direction and simple shearing; θ' is the angle between the long axis of finite strain ellipse and deformation zone. The W_{k_i} lines can be considered as deformation paths for steady-state deformations.

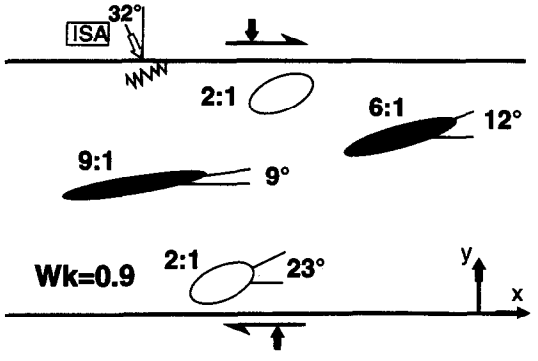

Fig. 9. Fictitious shear zone with instantaneous (e.g. stylolites) and finite strain markers (ellipses), from which W_{k_i} can be determined. Finite strain ellipses indicate elliptical ratio and orientation from the shear plane.

measurements should plot along a constant W_{k_i} curve (e.g. Fig. 8a for sub-simple shearing). If they do not, as in the case demonstrated by Srivastava *et al.* (1995), then the W_{k_i} simply represents an average kinematic vorticity number for the deformation.

Porphyroblasts

Because the vorticity vector may be interpreted as twice the rate of rotation of a rigid spherical inclusion in a ductile matrix, rigid spherical inclusions may be used to obtain an approximate estimate of the vorticity (Ghosh 1987). In this case, the rotation Ω of the inclusion must be extracted from the rock, e.g. by looking at inclusion patterns in garnets (Vissers 1989). For steady-state, plane strain deformations, $\gamma = 2\Omega$. Combined with a strain estimate from the matrix, an approximate estimate may be obtained for intermediate–low W_{k_i} deformations by using equation (6) in Ghosh (1987). However, a more exact estimate may be obtained using the equation

$$W_{k_i} = \frac{\gamma}{\sqrt{2\{\ln(1+\Delta)^2\} + (\gamma)^2}} \qquad (17)$$

(Appendix C) if the volume change can be determined from independent means, e.g. chemical analyses. Similarly, W_{k_i} may be determined for a sub-simple shear deformation [using equation (11)] if the pure shear component ($k_1 = 1/k_2$) can be extracted from the deformed wall rocks.

Passchier (1987) emphasized that the orientation of immobilized (non-rotating) porphyroblasts/clasts with respect to the shear plane is a function of W_{k_i}, the shape of the clasts and the ratio of the ISA. Therefore, knowledge of which clasts remain immobilized allows estimation of W_{k_i}. The method is not very accurate for naturally deformed rocks, probably due to heterogeneity, local strain partitioning, and slip along the particle boundaries.

Deformed sets of dikes or veins

Deformed sets of veins and dikes represent another potential means for extracting W_{k_i} from rocks, since such objects variably record their respective stretch history (Talbot 1970, Hutton 1982). By mapping the various geometric sectors of the same deformation history (boudinaged then folded, etc.), Passchier (1990) shows how W_{k_i} can be estimated, even if the finite state of strain is unknown (also see Wallis 1992). The main assumptions are steady state sub-simple shearing and/or volume change deformation.

Passchier & Urai (1988) combined information from fibers and veins for vorticity analysis. By studying the relative rotation of pre-existing veins and extracting ISA from fiber orientation, they obtained an estimate for W_{k_i}.

Crystallographic fabrics

Wallis (1992) used the assumption that the central girdle of quartz *c*-axis diagrams develops perpendicular to the shear plane (i.e. AP_1) in sub-simple shearing. Together with independent estimates of finite strain, he obtained an estimate of W_{k_i}. The assumptions include steady-state, plane strain deformation with no volume change, in addition to the relationship between crystallographic fabric and the shear plane. Law *et al.* (1984) and Schmid & Casey (1986) also attempted similar methods of correlating quartz fabrics to vorticity. Due to the uncertainties in crystallographic fabric development, this method is perhaps best considered as semi-quantitative.

Calcite *c*-axis shows slightly more hopeful results of correlating vorticity to petrofabric development. Wenk *et al.* (1987) used the obliquity of the (0001) maximum or *c*-axis of calcite, relative to the shear plane, to determine the W_{k_i} of deformation. This type of analysis was subsequently applied to other field examples (e.g. Erskine *et al.* 1993). As pointed out in these analyses, potential problems such as strain partitioning must be addressed when correlating this type of analysis to an entire zone.

Tension gashes and fibers

Tension gashes and fibers may provide information about the ISA, and its angle to the shear zone may give an accurate and simple estimate of W_{k_i} (Fossen & Tikoff 1993). This method is based on the relationship between the ISA and W_{k_i}. However, it is necessary to assume a particular type of two- or three-dimensional deformation, applying different formulas or graphs in each case. For combinations of sub-simple shearing, Fig. 8(a) may be applied; for combinations of simple shear and volume change across the shear zone, Fig. 8(b) is appropriate; and for transpression/transtension, Fig. 7(a) is appropriate. If a deformation 'type' can be identified, then a three-dimensional vorticity number can be obtained.

An example is given in Fig. 7, based on studies by Jackson & Sanderson (1991), Jackson (1991), and Tikoff & Teyssier (1992). In these studies, an échelon veins

were considered to form in transtensional and transpressional deformations. The veins were assumed to open in the $\dot{s}_1$ direction and the fracture tip was oriented in either $\dot{s}_2$ or $\dot{s}_3$ direction (corroborated by the occurrence of stylolite peaks). Using fracture tips and the orientation of the shear zone boundary, W_{k_i} can be determined (Fig. 7a). In this case, the boundary conditions (e.g. transpression) of deformation can also be corroborated. Both Jackson & Sanderson (1991) and Tikoff & Teyssier (1992) noticed that en échelon fracture sets rarely form at greater than 55° from the shear zone boundary at the studied locality. Notice that the $\dot{s}_1$ direction becomes vertical for transpressional cases if $W_{k_i} < 0.81$ (i.e. pure, shear-dominated transpression), corresponding to the case where $\dot{s}_3$ is oriented at greater than 55° to the shear zone boundary. Therefore, the boundary conditions of deformation (e.g. transpression) can also be determined by judicious use of strain data (Fossen *et al.* 1994).

Porphyroclast interaction

Tikoff and Teyssier (1994a) used the interaction of porphyroclasts to estimate W_{k_i}. Their vorticity analysis is based on both the differential rotation of elliptical clasts and particle paths for deformations of different W_{k_i} values. The result is that fewer clasts tend to imbricate during high W_{k_i} sub-simple shearing, since imbricated clasts (which are being held together by their particle paths) rotate quickly in simple shearing-dominated deformation and become mutually independent. Therefore, knowledge of finite strain and number of imbricated clasts can provide an estimate of W_{k_i}. The authors also use a shape fabric of the elliptical clasts to corroborate their W_{k_i} estimate from imbrication.

DISCUSSION

The basic assumptions involved in all the aforementioned vorticity analyses will always impose a significant amount of uncertainty in vorticity estimates. Particularly questionable is the assumption of steady-state deformation which, in most cases, is inevitable. The best justification of steady-state deformation is one of constant boundary conditions, particularly movement of material particles or orientation of flow apophyses. If a deformation is driven by a kinematic process, for example plate motion, that is relatively constant over sufficient time to create deformation, then the assumption of steady-state deformation is justified as a first-order approximation.

However, as methods for determining W_{k_i} from naturally deforming rocks become more sophisticated, the exact nature of deformation history—and perhaps the controlling factors in deformation zones—will become better known. A major challenge in this respect is to be able to retrieve as much information, with as few assumptions as possible, about the strain history of naturally deformed rocks.

CONCLUSION

The internal kinematic vorticity number (W_{k_i}) may be a useful tool in two-dimensional structural analysis, but in most three-dimensional deformations W_{k_i} becomes less precise and thus less useful. Some commonly made assumptions for two-dimensional deformation are therefore not applicable to three-dimensional deformations. For example, neither the orientation of the flow apophyses nor instantaneous strain axes, with respect to the shear zone boundary, result in knowledge of W_{k_i}. In three dimensions, the recognition of the 'type' of deformation—i.e. transpression (*stricto sensu*) vs flattening with an orthogonal simple shearing—in addition to a W_{k_i} estimate is necessary to describe deformation. Therefore, vorticity analysis in three dimensions must also include a qualitative description of the deformation, exhibiting the importance of boundary conditions in geological processes.

The mathematics derived in this paper is applied to finding practical ways of determining W_{k_i} from naturally deformed rocks. Knowledge of the orientation of the flow apophyses or ISA can often be used to determine W_{k_i} and/or constrain the boundary conditions of deformation. Gradients in finite strain are also capable of determining W_{k_i} and boundary conditions, if steady-state deformation is assumed. Steady-state deformation is best justified as a first-order approximation if kinematic processes are constant over sufficient time to create deformation. The assumption of steady-state deformation is unlikely for many geological settings, but can be tested using some of the methods outlined above.

Acknowledgements—This work was supported by a University of Minnesota Doctoral Dissertation Fellowship and NSF EAR-9305262 for B.T. P. Hudleston, C. Teyssier and S. Wojtal are thanked for helpful conversations. S. Treagus, C. Passchier and an anonymous reviewer are also acknowledged for suggesting significant improvements to this paper.

REFERENCES

Bobyarchick, A. R. 1986. The eigenvalues of steady flow in Mohr space. *Tectonophysics* **122**, 35–51.

Dennis, A. J. & Secor, D. T. 1990. On resolving shear direction in foliated rocks deformed by simple shear. *Bull. geol. Soc. Am.* **102**, 1257–1267.

De Paor, D. G. & Means, W. D. 1984. Mohr circles of the first and second kind and their use to represent tensor operations. *J. Struct. Geol.* **6**, 693–701.

Elliott, D. 1972. Deformation paths in structural geology. *Bull. geol. Soc. Am.* **83**, 2621–2635.

Erickson, J. L. 1960. Appendix on tensor fields. In: *The Classic Field Theories, Encyclopedia of Physics* (edited by Flugge, S.). Springer, Berlin, pp. 226–858.

Erskine, B. G., Heidelbach, F. & Wenk, W.-R. 1993. Lattice preferred orientations and microstructures of deformed Cordilleran marbles: correlation of shear indicators and determination of strain path. *J. Struct. Geol.* **15**, 1189–1205.

Flinn, D. 1979. The deformation matrix and the deformation ellipsoid. *J. Struct. Geol.* **1**, 299–307.

Fossen, H. & Tikoff, B. 1993. The deformation matrix for simultaneous simple shearing, pure shearing, and volume change, and its application to transpression/transtension tectonics. *J. Struct. Geol.* **15**, 413–422.

Fossen, H., Tikoff, B. & Teyssier, C. 1994. Strain modeling of transpressional and transtensional deformation. *Norsk geol. Tidsskr.* **74**, 134–145.
Ghosh, S. K. 1987. Measure of non-coaxiality. *J. Struct. Geol.* **9**, 111–113.
Hutton, D. H. W. 1982. A tectonic model for the emplacement of the Main Donegal Granite, NW Ireland. *J. geol. Soc. Lond.* **139**, 615–631.
Jackson, R. R. 1991. Vein arrays and their relationship to transpression during fold development in the Culm Basin, central south-west England. *Ann. Conf. Ussher Soc.* 356–362.
Jackson, R. R. & Sanderson, D. J. 1991. Transtensional modeling of en échelon vein arrays. *Mitt. aus den Geol. Inst. ETH Zurich* **239b**, 166–167.
Kirby, S. H. & Kronenberg. 1987 Rheology of the lithosphere: selected topics. *Rev. Geophys.* **25/6**, 1219–1244.
Kreyszig, E. 1972. *Advanced Engineering Mathematics*. Third edition. John Wiley & Sons, London, 866 pp.
Law, R. D., Knipe, R. J. & Dayan, H. 1984. Strain path partitioning within thrust sheets: microstructural and petrofabric evidence from the Moine thrust at Loch Eriboll, northwest Scotland. *J. Struct. Geol.* **6**, 477–497.
Lister, G. S. & Williams, P. F. 1983. The partitioning of deformation in flowing rock masses. *Tectonophysics* **92**, 1–33.
Malvern, L. E. 1969. *Introduction to the Mechanics of a Continuous Medium*. Prentice-Hall, Englewood Cliffs, New Jersey.
McKenzie, D. 1979. Finite deformation during fluid flow. *Geophys. J. R. astr. Soc.* **58**, 689–715.
Means, W. D. 1983. An unfamiliar Mohr circle construction for finite strain. *Tectonophysics* **89**, T1–T6.
Means, W. D. 1990. Kinematics, stress, deformation and material behaviour. *J. Struct. Geol.* **12**, 953–971.
Means, W. D., Hobbs, B. E., Lister, G. S. & Williams, P. F. 1980. Vorticity and non-coaxiality in progressive deformations. *J. Struct. Geol.* **2**, 371–378.
Merle, O. 1986. Patterns of stretch trajectories and strain rates within spreading–gliding nappes. *Tectonophysics* **124**, 211–222.
Neurath, C. & Smith, R. B. 1982. The effect of material properties on growth rates of folding and boudinage: experiments with wax models. *J. Struct. Geol.* **4**, 215–229.
Passchier, C. W. 1987. Stable positions of rigid objects in non-coaxial flow—a study in vorticity analysis. *J. Struct. Geol.* **9**, 679–690.
Passchier, C. W. 1988a. The use of Mohr circles to describe non-coaxial progressive deformation. *Tectonophysics* **149**, 323–338.
Passchier, C. W. 1988b. Analysis of deformation paths in shear zones. *Geol. Rdsch.* **77**, 309–318.
Passchier, C. W. 1990. Reconstruction of deformation and flow parameters from deformed vein sets. *Tectonophysics* **180**, 185–199.
Passchier, C. W. & Urai, J. L. 1988. Vorticity and strain analysis using Mohr diagrams. *J. Struct. Geol.* **10**, 755–763.
Pfiffner, O. A. & Ramsay, J. G. 1982. Constraints on geological strain rates: arguments from finite strain states of naturally deformed rocks. *J. geophs. Res.* **87**, 311–321.
Ramberg, H. 1975a. Particle paths, displacement and progressive strain applicable to rocks. *Tectonophysics* **28**, 1–37.
Ramberg, H. 1975b. Superposition of homogeneous strain and progressive deformation in rocks. *Bull. geol. Inst. Uppsala* **6**, 35–67.
Robin, P.-Y. F. & Cruden, A. R. 1994. Strain and vorticity patterns in ideally ductile transpression zones. *J. Struct. Geol.* **16**, 447–466.
Sanderson, D. J. 1976. The superposition of compaction and plane strain. *Tectonophysics* **30**, 35–54.
Schmid, S. M. & Casey, M. 1986. Complete fabric analysis of some commonly observed quartz *c*-axis patterns. In: *Mineral and Rock Deformation: Laboratory Studies (The Paterson Volume)* (edited by Hobbs, B. E. & Heard, H. C.). *Am. geophys. Un. geophys. Monogr.* **36**, 263–286, Washington.
Simpson, C. & De Paor, D. G. 1993. Strain and kinematic analysis in general shear zones. *J. Struct. Geol.* **15**, 1–20.
Srivastava, H. B., Hudleston, P. & Earley, D. 1995. Strain and volume loss in a ductile shear zone. *J. Struct. Geol.* **17**, 1217–1231.
Talbot, C. J. 1970. The minimum strain ellipsoide using deformed quartz veins. *Tectonophysics* **9**, 47–76.
Tikoff, B. & Fossen, H. 1993. Simultaneous pure and simple shear: the unified deformation matrix. *Tectonophysics* **217**, 267–283.
Tikoff, B. & Teyssier, C. 1992. En échelon vein sets and *P*-fractures as indicators of transpressional zones in deformed limestone. *Geol. Soc. Am. Abs. W. Progr.* p. A322.
Tikoff, B. & Teyssier, C. 1994a. Strain and fabric analyses based on porphyroclast interaction. *J. Struct. Geol.* **16**, 477–491.
Tikoff, B. & Teyssier, C. 1994b. Strain modeling of displacement field partitioning in transpressional orogens. *J. Struct. Geol.* **16**, 1575–1588.
Truesdell, C. 1953. Two measures of vorticity. *J. Rational Mech. Anal.* **2**, 173–217.
Vissers, R. L. M. 1989. Asymmetric quartz *c*-axis fabrics and flow vorticity: a study using rotated garnets. *J. Struct. Geol.* **11**, 231–244.
Wallis, S. R. 1992. Vorticity analysis in metachert from the Sanbagawa Belt, SW Japan. *J. Struct. Geol.* **14**, 271–280.
Weijermars, R. 1991. The role of stress in ductile deformation. *J. Struct. Geol.* **13**, 1061–1078.
Wenk, W.-R., Takeshita, T., Bechler, E., Erskine, B. G. & Matthies, S. 1987. Pure shear and simple shear calcite fabrics. Comparison of experimental, theoretical and natural data. *J. Struct. Geol.* **9**, 731–745.
White, S. H., Burrows, S. E., Carreras, J., Shaw, N. D. & Humphreys, F. J. 1980. On mylonites in ductile shear zones. *J. Struct. Geol.* **2**, 175–187.

APPENDIX A

Continuum mechanics framework

A velocity field given by

$$\mathbf{L} = \begin{pmatrix} \dot{\varepsilon}_x & \dot{\gamma}_{xy} & \dot{\gamma}_{xz} \\ \dot{\gamma}_{yx} & \dot{\varepsilon}_y & \dot{\gamma}_{yx} \\ \dot{\gamma}_{zx} & \dot{\gamma}_{zy} & \dot{\varepsilon}_z \end{pmatrix}, \tag{A1}$$

can be decomposed into the stretching tensor $\dot{\mathbf{S}}$ and the vorticity tensor $\mathbf{W}$, given by the equations

$$\dot{\mathbf{S}} = \begin{bmatrix} \dot{\varepsilon}_x & \frac{1}{2}(\dot{\gamma}_{xy} + \dot{\gamma}_{yx}) & \frac{1}{2}(\dot{\gamma}_{xz} + \dot{\gamma}_{zx}) \\ \frac{1}{2}(\dot{\gamma}_{xy} + \dot{\gamma}_{yx}) & \dot{\varepsilon}_y & \frac{1}{2}(\dot{\gamma}_{yz} + \dot{\gamma}_{zy}) \\ \frac{1}{2}(\dot{\gamma}_{xz} + \dot{\gamma}_{zx}) & \frac{1}{2}(\dot{\gamma}_{yz} + \dot{\gamma}_{zy}) & \dot{\varepsilon}_z \end{bmatrix} \tag{A2}$$

and

$$\mathbf{W} = \begin{bmatrix} \dot{\varepsilon}_x & \frac{1}{2}(\dot{\gamma}_{xy} - \dot{\gamma}_{yx}) & \frac{1}{2}(\dot{\gamma}_{xz} - \dot{\gamma}_{zx}) \\ \frac{1}{2}(\dot{\gamma}_{yx} - \dot{\gamma}_{xy}) & \dot{\varepsilon}_y & \frac{1}{2}(\dot{\gamma}_{yz} - \dot{\gamma}_{zy}) \\ \frac{1}{2}(\dot{\gamma}_{zx} - \dot{\gamma}_{xz}) & \frac{1}{2}(\dot{\gamma}_{zy} - \dot{\gamma}_{yz}) & \dot{\varepsilon}_z \end{bmatrix}. \tag{A3}$$

Writing out the velocity field in equation form, we get:

$$\begin{aligned} v_1 &= \dot{\varepsilon}_x x + \dot{\gamma}_{xy} y + \dot{\gamma}_{xz} z \\ v_2 &= \dot{\gamma}_{yx} x + \dot{\varepsilon}_y y + \dot{\gamma}_{yz} z \\ v_3 &= \dot{\gamma}_{zx} x + \dot{\gamma}_{zy} y + \dot{\varepsilon}_z z. \end{aligned} \tag{A4}$$

The vorticity vector $\mathbf{w}$ is defined as the curl of the velocity field $\mathbf{v}$. Therefore, for our three-dimensional deformation, the vorticity vector is

$$\mathbf{w} = \begin{pmatrix} \dot{\gamma}_{zy} - \dot{\gamma}_{yz} \\ \dot{\gamma}_{xz} - \dot{\gamma}_{zx} \\ \dot{\gamma}_{yx} - \dot{\gamma}_{xy} \end{pmatrix}, \tag{A5}$$

and its magnitude is therefore

$$w = \sqrt{(\dot{\gamma}_{zy} - \dot{\gamma}_{yz})^2 + (\dot{\gamma}_{xz} - \dot{\gamma}_{zx})^2 + (\dot{\gamma}_{yx} - \dot{\gamma}_{xy})^2}. \tag{A6}$$

To find the principal strain rates, we follow the analysis of Means *et al.* (1980), who define the kinematic vorticity number as

$$W_k = \frac{w}{\sqrt{2(S_1^2 + S_2^2 + S_3^2)}} = \frac{w}{\sqrt{2\Pi}}, \tag{A7}$$

where Π is the invariant second moment of the stretching tensor (Erikson 1960). Using the stretching tensor $\dot{\mathbf{S}}$ [equation (A2)] we can find Π from the relationship (Means *et al.* 1980):

$$\begin{aligned} \Pi = \text{trace}\,(\dot{S}\dot{S}^T) &= \dot{\varepsilon}_x^2 + \dot{\varepsilon}_y^2 + \dot{\varepsilon}_z^2 \\ &+ \tfrac{1}{2}[(\dot{\gamma}_{xy} + \dot{\gamma}_{yx})^2 + (\dot{\gamma}_{xz} + \dot{\gamma}_{zx})^2 + (\dot{\gamma}_{yz} + \dot{\gamma}_{zy})^2]. \end{aligned} \tag{A8}$$

The kinematic vorticity number can thus be written as

$$W_k = \frac{\sqrt{(\dot{\gamma}_{zxy} - \dot{\gamma}_{yz})^2 + (\dot{\gamma}_{xz} - \dot{\gamma}_{zx})^2 + (\dot{\gamma}_{yx} - \dot{\gamma}_{xy})^2}}{\sqrt{2(\dot{\varepsilon}_x^2 + \dot{\varepsilon}_y^2 + \dot{\varepsilon}_z^2) + [(\dot{\gamma}_{xy} + \dot{\gamma}_{yx})^2 + (\dot{\gamma}_{xz} + \dot{\gamma}_{zx})^2 + (\dot{\gamma}_{yz} + \dot{\gamma}_{zy})^2]}}. \quad \text{(A9)}$$

For the case of an upper triangular velocity gradient matrix, as given in equation (5), the expression for W_{k_i} can be simplified to

$$W_{k_i} = \frac{\sqrt{(\dot{\gamma}_{yz})^2 + (\dot{\gamma}_{xz})^2 + (\dot{\gamma}_{xy})^2}}{\sqrt{2(\dot{\varepsilon}_x^2 + \dot{\varepsilon}_y^2 + \dot{\varepsilon}_z^2) + (\dot{\gamma}_{xy})^2 + (\dot{\gamma}_{xz})^2 + (\dot{\gamma}_{yz})^2}}. \quad \text{(A10)}$$

To relate this number to the actual components of pure and simple shear, we use the substitutions of (8) and obtain

$$W_{k_i} = \frac{\sqrt{(\gamma_{yz})^2 + (\gamma_{xz})^2 + (\gamma_{xy})^2}}{\sqrt{2[\ln(k_1)^2 + \ln(k_2)^2 + \ln(k_3)^2] + (\gamma_{xy})^2 + (\gamma_{xz})^2 + (\gamma_{yz})^2}}. \quad \text{(A11)}$$

The eigenvectors and eigenvalues of the velocity gradient tensor define the orientation and magnitude of the three flow apophyses (Bobyarchick 1986). As eigenvectors of **L**, the flow apophyses are orientations in space that represent the maximum, minimum and intermediate gradients of particle motion defined at an instant. The motion of all material points along the flow apophyses is either directly toward, away from, or fixed with respect to the origin. For an upper triangular deformation matrix [equation (5)], the magnitude of the flow apophyses (eigenvalues of **L**) are simply the instantaneous pure shear rates, and their orientations (eigenvectors of **L**) are

$$\begin{bmatrix} 1 \\ 0 \\ 0 \end{bmatrix}, \begin{bmatrix} \frac{-\dot{\gamma}_{xy}}{\dot{\varepsilon}_x - \dot{\varepsilon}_y} \\ 1 \\ 0 \end{bmatrix}, \begin{bmatrix} \frac{\dot{\gamma}_{xz}}{\dot{\varepsilon}_x - \dot{\varepsilon}_z} + \frac{\dot{\gamma}_{xy}\dot{\gamma}_{yz}}{(\dot{\varepsilon}_x - \dot{\varepsilon}_z)(\dot{\varepsilon}_y - \dot{\varepsilon}_z)} \\ \frac{-\dot{\gamma}_{yz}}{\dot{\varepsilon}_y - \dot{\varepsilon}_z} \\ 1 \end{bmatrix} \quad \text{(A12)}$$

(Tikoff and Fossen 1993). The first apophysis is always parallel to the x-axis and the second lies in the x–y plane, but generally inclined to both axes. The last apophysis is generally inclined to all three axes, although, for a two-dimensional deformation ($\gamma_{xz} = \gamma_{yz} = 0$), the flow apophysis is parallel to the z-axis. Since **L** is not a symmetric matrix, the eigenvectors (flow apophyses) are not necessarily mutually perpendicular.

The eigenvectors and eigenvalues of the stretching tensor $\dot{\mathbf{S}}$ define the orientation and magnitude of the instantaneous stretching axes (e.g. Passchier 1988b) or instantaneous strain axes (Tikoff & Teyssier 1994b), in either case referred to as the ISA (Malvern 1969, Lister & Williams 1983). The ISAs represent the direction of maximum, intermediate and minimum change of material line length in an instant. The eigenvalues give the rate of stretching of these material lines. Because $\dot{\mathbf{S}}$ is symmetric, the eigenvectors, or ISA orientations, are mutually perpendicular. These values are best solved numerically for three-dimensional deformations.

However, analytical expressions for the magnitude and orientation of the ISA are appropriate for two-dimensional deformations. For $\dot{\mathbf{S}}$ given by

$$\dot{\mathbf{S}} = \begin{bmatrix} \dot{\varepsilon}_x & \frac{1}{2}\dot{\gamma} \\ \frac{1}{2}\dot{\gamma} & \dot{\varepsilon}_y \end{bmatrix}, \quad \text{(A13)}$$

the eigenvalues are given by the equations

$$\dot{s}_{1,2} = \frac{(\dot{\varepsilon}_x + \dot{\varepsilon}_y) \pm \sqrt{(\dot{\varepsilon}_x + \dot{\varepsilon}_y)^2 - 4\left(\dot{\varepsilon}_x\dot{\varepsilon}_y - \frac{\dot{\gamma}^2}{4}\right)}}{2}$$

$$= \frac{(\dot{\varepsilon}_x + \dot{\varepsilon}_y) \pm \sqrt{(\dot{\varepsilon}_x - \dot{\varepsilon}_y)^2 + \dot{\gamma}^2}}{2} \quad \text{(A14)}$$

The eigenvectors of $\dot{\mathbf{S}}$ can be found by inserting the eigenvalues into the stretching tensor. These eigenvectors must satisfy the equation

$$(\dot{\mathbf{S}} - \dot{s}_{\max} I)\mathbf{e} = \begin{bmatrix} \dot{\varepsilon}_x - \dot{s}_{\max} & \frac{\dot{\gamma}}{2} \\ \frac{\dot{\gamma}}{2} & \dot{\varepsilon}_y - \dot{s}_{\max} \end{bmatrix} \begin{bmatrix} x \\ y \end{bmatrix} = 0, \quad \text{(A15)}$$

where $\mathbf{e}$ is an eigenvector. We can restrict our interest only to $s_{\max}$, since we only need to know the orientation of the long axis of the finite strain ellipse. Multiplying out equation (A15), we get

$$(\dot{\varepsilon}_x - \dot{s}_{\max})x + \frac{\dot{\gamma}}{2}y = 0, \quad \text{(A16a)}$$

and

$$\frac{\dot{\gamma}}{2}x + (\dot{\varepsilon}_y - \dot{s}_{\max})y = 0. \quad \text{(A16b)}$$

Using equation (A16) and $\tan\theta = y/x$, the angle between the long axis of the instantaneous strain or extensional ISA (corresponding to the largest eigenvalue of $\dot{\mathbf{S}}$) and the positive x-axis, is

$$\frac{y}{x} = \tan\theta = \frac{-2}{\dot{\gamma}}(\dot{\varepsilon}_x - \dot{s}_{\max}) \quad \text{(A17a)}$$

or

$$\theta = \arctan\left\{\frac{-2}{\dot{\gamma}}\left[\dot{\varepsilon}_x - \frac{(\dot{\varepsilon}_x + \dot{\varepsilon}_y) \pm \sqrt{(\dot{\varepsilon}_x - \dot{\varepsilon}_y)^2 + \dot{\gamma}^2}}{2}\right]\right\}. \quad \text{(A17b)}$$

Using the time-independent relationships given in equation (8), which assume a steady-state deformation, one can express instantaneous strain quantities in terms of finite strain components of the deformation matrix.

APPENDIX B

Comparison of two-dimensional and three-dimensional deformation

We compare two- and three-dimensional deformations by using comparable components of pure shear ($k_1/k_3 = 4$) and a simple shear ($\gamma = 1$) in the plane which contains the long and short axes of the finite strain ellipsoid. This two-dimensional, sub-simple shearing deformation gives a $W_{k_i} = 0.585$ using equation (10). The three-dimensional deformations must be calculated in a more complicated procedure.

Pure constriction

In the case of pure constriction, we have the conditions

$$\gamma_T = 1, \quad k_1 > k_2 = k_3, \quad k_1k_2k_3 = 1, \quad \text{and} \quad k_1/k_3 = 4. \quad \text{(B1)}$$

Combining these conditions gives

$$k_3 = (0.25)^{1/3} = 0.630, \quad k_2 = 0.630, \quad k_1 = 2.52, \quad \text{(B2)}$$

and, using equation (10), $W_{k_i} = 0.530$.

Pure flattening

For pure flattening, we have

$$\gamma_T = 1, \quad k_1k_2k_3 = 1, \quad k_1 = k_2 > k_3, \quad \text{and} \quad k_1/k_3 = 4. \quad \text{(B3)}$$

Combining these conditions gives

$$k_1 = 4^{1/3} = 1.5874, \quad k_2 = 1.5874, \quad k_3 = 0.39685, \quad \text{(B4)}$$

and $W_{k_i} = 0.530$.

Notice that the effective shear, Γ, is different for the three cases:

$$\Gamma_{\text{two-dimensional}} = 1.08, \quad \Gamma_{\text{flattening}} = 1.36 \quad \text{and} \quad \Gamma_{\text{constriction}} = 0.85,$$

as are the dimensions of the axes of the finite strain ellipse:

$$\lambda_{\text{max—two-dimensional}} = 5.22, \quad \lambda_{\text{min—two-dimensional}} = 0.191,$$

$$\lambda_{\text{max—constriction}} = 8.30, \quad \lambda_{\text{min—constriction}} = 0.303,$$

$$\lambda_{\text{max—flattening}} = 3.29, \quad \text{and} \quad \lambda_{\text{min—flattening}} = 0.120.$$

However, the finite strain ellipse ratio in a vertical plane that contains the long and short axis of the finite strain ellipse is the same for all these cases, $R = 27.35$, and a direct comparison can be made.

APPENDIX C

Anisotropic volume loss

Anisotropic volume loss can be thought of as a compressive pure shear component of deformation that is not compensated for by

extension (Sanderson 1976). For a two-dimensional, steady-state deformation involving simultaneous volume loss and simple shearing, the velocity gradient tensor is given by:

$$\mathbf{L} = \begin{bmatrix} 0 & \dot{\gamma} \\ 0 & \dot{\delta} \end{bmatrix}, \tag{C1}$$

where $\dot{\delta}$ is the instantaneous volume loss rate and $\dot{\gamma}$ is the simple shear strain rate. Using the relations

$$\dot{\gamma} = \gamma/t$$

and

$$\exp(\dot{\delta}t) = 1 + \Delta, \tag{C2}$$

and assuming a steady-state deformation, a general deformation matrix (position gradient tensor) is

$$\mathbf{D} = \begin{bmatrix} 1 & \dfrac{\gamma\Delta}{\ln(1+\Delta)} \\ 0 & 1+\Delta \end{bmatrix} \tag{C3}$$

(Fossen & Tikoff 1993), where Δ represents anisotropic volume change. The kinematic vorticity number for anisotropic volume loss acting perpendicular to a simple shear component is

$$W_{k_i} = \frac{\gamma}{\sqrt{2\{\ln(1+\Delta)^2\} + (\gamma)^2}}. \tag{C4}$$

Using these relations, it becomes possible to correlate finite strain and W_{k_i}, as shown in Fig. 8(b). Anisotropic volume loss affects vorticity estimates. For a given orientation of the flow apophysis, the W_{k_i} value is always lower for anisotropic volume loss and simple shearing compared to sub-simple shearing. Because the former case does not elongate material parallel to the x-direction, the rotation of material lines is slower—and thus W_{k_i} is lower—when the flow apophyses are identical. An alternative way of stating this relationship is that the extensional ISA is oriented closer to the x-direction for a given W_{k_i} value for sub-simple shearing. For example, compare the $R = 1$ values for $W_{k_i} = 0.9$ for the case of sub-simple shearing (32°; Fig. 8a) and anisotropic volume loss and simple shear (36°; Fig. 8b). As for the case of sub-simple shearing, a given W_{k_i} value corresponds to either volume loss or gain in the y-direction, thereby explaining the two W_{k_i} values in Fig. 8(b).